

# Extracellular Vesicles Maintain Blood-Brain Barrier Integrity by the Suppression of Caveolin-1/CD147/VEGFR2/MMP Pathway After Ischemic Stroke

Yiyang Li<sup>1,\*</sup>, Jiali Chen<sup>1,\*</sup>, Xingping Quan<sup>1</sup>, Ying Chen<sup>2</sup>, Yan Han<sup>1</sup>, Jinfen Chen<sup>1</sup>, Li Yang<sup>1</sup>, Youhua Xu<sup>3</sup>, Xu Shen<sup>4</sup>, Ruibing Wang<sup>1,5</sup>, Yonghua Zhao<sup>1,5</sup>

<sup>1</sup>Institute of Chinese Medical Sciences, State Key Laboratory of Quality Research in Chinese Medicine, University of Macau, Taipa, Macao SAR, People's Republic of China; <sup>2</sup>School of Health Economics and Management, Nanjing University of Chinese Medicine, Nanjing, Jiangsu, People's Republic of China; <sup>3</sup>Faculty of Chinese Medicine, Macau University of Science and Technology, Taipa, Macao SAR, People's Republic of China; <sup>4</sup>Jiangsu Key Laboratory of Drug Target and Drug for Degenerative Diseases, Nanjing University of Chinese Medicine, Nanjing, People's Republic of China; <sup>5</sup>Department of Pharmaceutical Sciences, Faculty of Health Sciences, University of Macau, Taipa, Macao SAR, People's Republic of China

\*These authors contributed equally to this work

Correspondence: Yonghua Zhao, Institute of Chinese Medical Sciences, State Key Laboratory of Quality Research in Chinese Medicine, University of Macau, Taipa, Macao SAR, People's Republic of China, Tel +853-88224877, Fax +853-28841358, Email yonghuazhao@um.edu.mo

**Background:** Ischemic stroke (IS) causes tragic death and disability worldwide. However, effective therapeutic interventions are finite. After IS, blood-brain barrier (BBB) integrity is disrupted, resulting in deteriorating neurological function. As a novel therapeutic, extracellular vesicles (EVs) have shown ideal restorative effects on BBB integrity post-stroke; however, the definite mechanisms remain ambiguous. In the present study, we investigated the curative effects and the mechanisms of EVs derived from bone marrow mesenchymal stem cells and brain endothelial cells (BMSC-EVs and BEC-EVs) on BBB integrity after acute IS.

**Methods:** EVs were isolated from BMSCs and BECs, and we investigated the therapeutic effect in vitro oxygen-glucose deprivation (OGD) insulted BECs model and in vivo rat middle cerebral artery occlusion (MCAo) model. The cell monolayer leakage, tight junction expression, and metalloproteinase (MMP) activity were evaluated, and rat brain infarct volume and neurological function were also analyzed.

**Results:** The administration of two kinds of EVs not only enhanced ZO-1 and Occludin expressions but also reduced the permeability and the activity of MMP-2/9 in OGD-insulted BECs. The amelioration of the cerebral infarction, BBB leakage, neurological function deficits, and the increasing ZO-1 and Occludin levels, as well as MMP activity inhibition was observed in MCAo rats. Additionally, the increased levels of Caveolin-1, CD147, vascular endothelial growth factor receptor 2 (VEGFR2), and vascular endothelial growth factor A (VEGFA) in isolated brain microvessels were downregulated after EVs treatment. In vitro, the employment of Caveolin-1 and CD147 siRNA partly suppressed the expressions of VEGFR2, VEGFA and MMP-2/9 activity and reduced the leakage of OGD insulted BECs and enhanced ZO-1 and Occludin expressions.

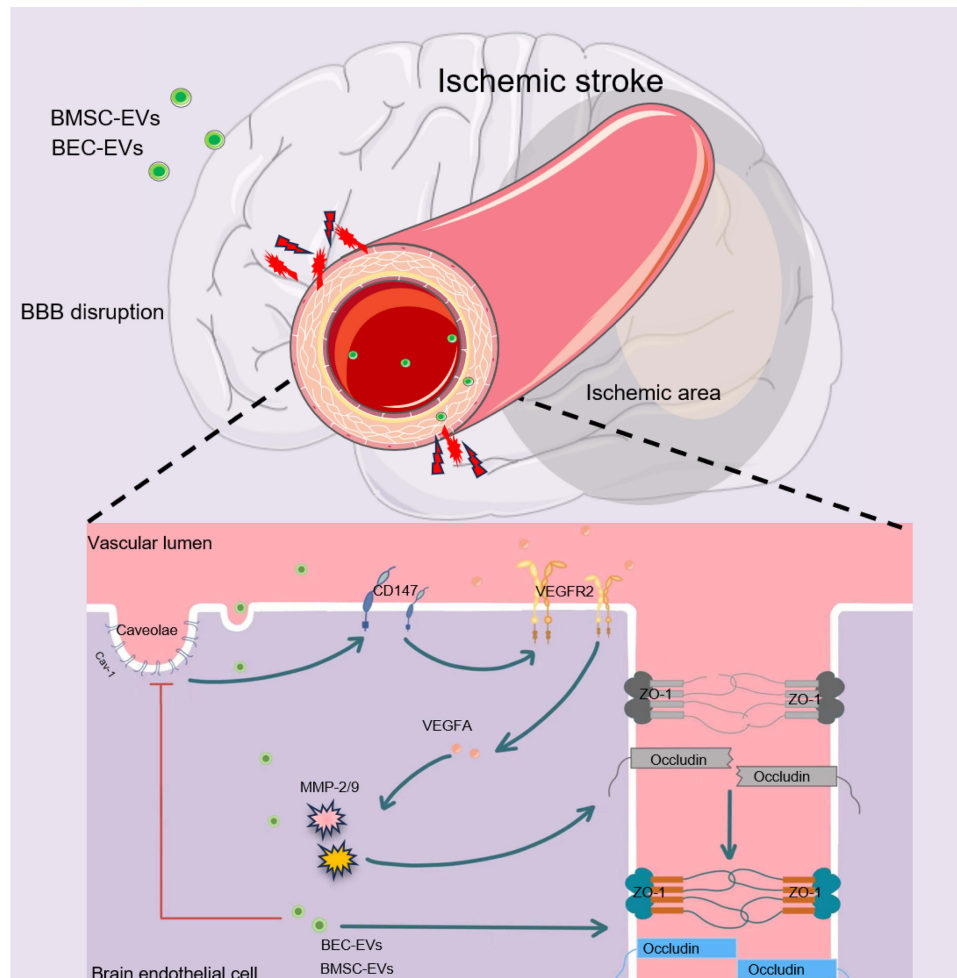
**Conclusion:** Our study firstly demonstrates that BEC and BMSC-EVs administrations maintain BBB integrity via the suppression of Caveolin-1/CD147/VEGFR2/MMP pathway after IS, and the efficacy of BMSC-EVs is superior to that of BEC-EVs.

**Keywords:** extracellular vesicles, ischemic stroke, Caveolin-1, CD147, matrix metalloproteinase, VEGFR2, blood-brain barrier

## Introduction

Acute ischemic stroke (IS) is a cerebrovascular event that disrupts normal cerebral blood flow and energy supply, followed by neurovascular unit dysfunctions, leading to neurological functional deficit. Miserably, IS displays a high risk in aging people, and in the US, three-quarters of stroke cases occurred in individuals over 65 years.<sup>1,2</sup> As the global aging acceleration in the population, stroke onset was increased by nearly 10% from the 1990s to 2010s, and the individual stroke risk doubled every ten years of age during a lifetime.<sup>3</sup> Among all the neurovascular impairments, blood-brain barrier (BBB) dysfunction is one predominant factor, which affects the pathological evolution risk and prognosis of IS patients. Physiologically, BBB plays

## Graphical Abstract



critical roles in separating peripheral blood from brain parenchyma, controlling substance exchange, and maintaining cerebral environment homeostasis. The integrity of BBB is damaged after IS onset, resulting in peripheral substances and immune cells entering the cerebral parenchyma. It exacerbates brain edema, inflammatory injury, and neurological outcome deficits.<sup>4,5</sup> Hence, the maintenance of BBB integrity is predominant to achieve a much better prognosis for IS patients.

Although numerous neuroprotective agents were reported to have positive effects on IS in pre-clinical studies, almost none were demonstrated to exert satisfactory actions in clinical trials.<sup>6,7</sup> Since 1996, the only FDA-approved clinical thrombolytic agent for IS treatment is recombinant tissue plasminogen activator (r-tPA),<sup>8</sup> but the potential side effects including intracranial hemorrhage, narrow therapeutic time window, various contraindications, and inpatient costs cause low administered rate.<sup>8–10</sup> Therefore, the development of innovative agents is imminent. Stem cell-based therapy has emerged as a promising approach for IS and has been applied to clinical trials, suggesting that neural stem cells and bone marrow mesenchymal stem cells (BMSCs) by intravenous administration have the potential to ameliorate neurological outcomes post-stroke.<sup>11</sup> However, it is necessary to be concerned that stem cell administration has some potential hazards, such as tumor formation, immune responses, and undesirable differentiation.<sup>12</sup> Recently, stem cells' paracrine extracellular vesicles (EVs) were reportedly to exert similar treatment effects on stroke to stem cells transplantation,<sup>13,14</sup> providing a new insight for IS treatment.

EVs are small phospholipid bilayer vesicles developed by all the cells via endosomal pathways, containing diverse biomolecules, such as non-coding nucleic acid, glycoproteins, and lipids.<sup>15</sup> It can cross BBB and be engulfed by cerebral cells.<sup>16,17</sup> Numerous studies have revealed that EVs from optimal cell origins exert diverse therapeutic functions, including neuroprotection, BBB integrity maintenance, cerebral inflammation regulation, and anti-apoptosis and autophagy intervention and so on after IS.<sup>18,19</sup> Hence, EVs treatment may be more predominant compared with stem cells transplantation therapy on IS. However, the exact therapeutic mechanisms of specific EVs on IS fails to be fully defined, although non-coding RNAs (miRNAs and circRNAs), proteomes, and lipids have been widely identified to facilitate the restoration after cerebral ischemia via extensive molecular biological pathways.<sup>20,21</sup>

CD147 is also named as extracellular matrix metalloproteinase inducer (EMMPRIN), which is a membrane protein expressed in plenty of cell types, and the expression and glycosylation of CD147 are responsible for the production of matrix metalloproteinases (MMP).<sup>22</sup> And MMP, especially MMP-2, and MMP-9, have been extensively demonstrated that they can degrade extracellular matrix (ECM), and damage tight junctions (TJs) between endothelial cells resulted in BBB permeability exacerbation, which aggravates the post-IS neurological functional deficits and inflammation activation.<sup>23–25</sup> CD147 has been first reported in cancer research to interact with MMP to facilitate tumor cells invasion and metastasis,<sup>26,27</sup> and in recent years, CD147 also been proved to regulate the progression of central nervous system diseases such as intracerebral hemorrhage<sup>28</sup> and stroke.<sup>25,29</sup> The detrimental role of CD147 in IS has been proved, and the inhibition of CD147 can alleviate neurological function deficits and inflammatory injury after IS in mice.<sup>25,30</sup> The definite mechanism of how CD147 contributes to the MMP generation has yet to be fully illustrated, but as an identified downstream of CD147,<sup>31,32</sup> vascular endothelial growth factor (VEGF) can directly facilitate the activation of MMP and enhanced the permeability of BBB resulted in hemorrhagic transformation (HT) after IS.<sup>33,34</sup> In addition, though no clear evidence suggests that CD147 can interact with VEGF pathway in MMP activation after IS, in breast cancer, malignant melanoma, and liver fibrosis, CD147 can intervene with VEGFR2/VEGFA dependent approach to accelerate the diseases progression. Hence, we hypothesize that CD147 might regulate VEGF pathway to induce MMPs activation after IS.

The interaction between CD147 and MMP was determined to be associated with their upstream Caveolin-1 (Cav-1).<sup>22</sup> As a scaffolding protein mainly located in cell membrane lipid-raft, Cav-1 phosphorylation at Tyr 14 regulates various signaling pathways involving VEGF, MMP, and reactive oxygen species (ROS) production during the progression of IS.<sup>35</sup> Additionally, it can also bind to the glycosylated CD147 in astrocytes and brain endothelial cells (BECs) to activate MMP-2/9, which aggregated BBB permeability and HT in diabetic IS rats with t-PA administration.<sup>36</sup> Therefore, intervening with the expression of Cav-1 and its downstream CD147, VEGF, and MMP may be an innovative pathway for the restoration of BBB integrity after IS.

In the current study, our results firstly demonstrated the therapeutic effect of BEC-EVs and BMSC-EVs on the maintenance of BBB integrity in oxygen-glucose deprivation (OGD)-treated BECs and rat MCAo model. Both EVs administrations can restore the expressions of tight junction ZO-1 and Occludin, reduce MMPs activity and significantly ameliorate neurological function deficit in MCAo rats. Further investigation revealed that the mechanism of BEC-EVs and BMSC-EVs treatments on BBB integrity is related to the suppression of Caveolin-1/CD147/VEGFR2/MMP pathway.

## Materials and Methods

### Separation of EVs

BEC (b. End3 cell line) and BMSC were both from Shanghai Zhong Qiao Xin Zhou Biotechnology Co., Ltd, whose EVs were extracted as previous described protocol with minor improvement<sup>37</sup> by using Exo-prep kit (HBM-EXP-C25, HansaBioMed Life Science) and purified by ultracentrifugation. Briefly, BMSCs and BECs were both seeded in 75 cm<sup>2</sup> flasks till 70–80% confluence. After that, the EVs-free medium was replaced, and cells were cultured for another 24 h until confluent. After collecting the supernatants by using 0.22 μm membrane filters (Millipore) and centrifugated at 2000 g for 10 mins to abandon the cell debris, the medium was further concentrated via ultrafiltration spin columns (28932358, Cytiva). Exo-prep reagent was added and left still for 1 h on ice. After centrifuging at 10,000 g under 4 °C, the EVs pellet was resuspended with PBS and then ultracentrifugated at 100,000 g for 120 mins by using a ultracentrifuge (XPN-100, Beckman Coulter) for further purification. The final purified BMSC-EVs and BEC-EVs were preserved in PBS and stored at –80 °C for next administration.

## EVs Characterization

To characterize BEC-EVs and BMSC-EVs, the size and concentration of EVs were evaluated by nanoparticle tracking analysis (NTA) device (Nanosight-NS500, Malvern Panalytical Ltd), and the morphological characteristics of EVs were observed by transmission electron microscope (TEM) (Service provided by Servicebio Inc.). The markers of EVs (ALIX, TSG 101, CD 9, and CD 63) were tested by Western blotting. The internalization of EVs by BEC was measured by using DiI labeled EVs. Briefly, 5  $\mu$ M DiI dye (V22885, Invitrogen) were incubated with EVs, and then washed by PBS with ultracentrifugation at 100,000 g for 120 mins. The isolated DiI labeled EVs were co-cultured with BECs under 37 °C for 120 mins. Thereafter, cells were fixed by 4% paraformaldehyde (PFA), and permeabilized by 0.5% Triton X-100. DAPI (C1005, Beyotime) was stained to visualize the nucleus, and then samples were observed by a confocal microscope (SP8, Leica).

## OGD Insulted BEC and EVs Treatment

BECs were cultured in Dulbecco's modified Eagle's medium (DMEM) (11965092, Gibco) with 10% fetal bovine serum (FBS) (26140079, Gibco) and 1% penicillin/streptomycin (15070063, Gibco). For standard culture environments, cells were maintained in an incubator with 95% O<sub>2</sub> and 5% CO<sub>2</sub> at 37°C. For OGD modeling, cell medium was replaced with glucose deprived DMEM (11966025, Gibco), and BEC-EVs and BMSC-EVs ( $1 \times 10^{10}$  particles, 100  $\mu$ g) were added into the medium of cultured BECs. BECs were then transferred to a hypoxic chamber (MIC-101, Billups-Rothenberg) for N<sub>2</sub> ventilation. The oxygen percentage in hypoxic chamber was kept at O<sub>2</sub>%  $\leq$ 0.5%, and OGD time lasted for 4 h at 37 °C.

## Transwell Assay

BECs were cultured into the upper chamber of a 24-well transwell plate in the density of  $5 \times 10^4$  per well. After incubation for 72 h, DMEM medium was replaced with medium containing 2 mg/mL TRITC-Dextran (4.4 kDa; T1037, Sigma-Aldrich). BEC-EVs and BMSC-EVs were dissolved in glucose deprived DMEM medium and added to the upper chamber in treatment groups, respectively. After OGD processing, 50  $\mu$ L medium from each upper and lower chamber was collected for fluorescence intensity detection by microplate reader (SpectraMax M5) at 550 nm excitation and 572 nm emission. After that, the permeability coefficient was determined as previously described:<sup>38</sup>

$$P_{\text{dextran}} = \left( \text{RFU}_{\text{lower chamber}} / \text{RFU}_{\text{upper chamber}} \right) (1/S)(V)(1/t).$$

“RFU”: the fluorescent intensity of the chambers; “S”: BEC monolayer surface area; “V”: the volume of lower chamber; “t”: the time that TRITC-dextran allowed to leak.

## Gelatin Zymography

Gelatin zymography was performed by using the detection kit (Real-Times, Beijing Biotechnology Co., Ltd.) followed by the kit protocol. Briefly, 1 mg protein extracted from cell samples was incubated with 1/10 sample volume of gelatin-sepharose 4B beads (17095601, GE Healthcare) overnight on ice to enrich MMPs. Afterward, the beads were washed by PBS 3 times, and resuspended in 40  $\mu$ L 10% dimethylsulfoxide for 30 mins. After centrifugation, the supernatant was collected, mixed with loading buffer, and electrophoretic separated in 10% sodium dodecyl sulfate (SDS) polyacrylamide gels containing 0.1% gelatin. MMPs standard control was loaded as MMPs positive control. The gels were then incubated with refolding buffer for 30 mins and developing buffer overnight. Finally, the gels were stained in Coomassie blue fast staining solution (P0017, Beyotime), and then destained in decolorizing solution (7% acetic acid and 5% methanol) for 2 h. The gels were then imaged by GelDoc MP Imaging System (Bio-Rad), and MMP bands were analyzed using image software.

## MCAo Model Establishment and EVs Administration

The animal experiment protocol was approved by the Ethics Committee of the University of Macau (Ethics number: UMARE-035–2020). The animal study was conducted according to the Guide for the Care and Use of Laboratory Animals (8th edition, Washington, D.C.: The National Academies Press, 2011). Male Sprague–Dawley (SD) rats (6–8 weeks, 250–280g) were anesthetized by intraperitoneally injection of 1.5% (w/v) pentobarbital sodium (30 mg/kg) before

they suffered from surgery. All rats were divided into four groups: SHAM, MCAo, BEC-EVs ( $1 \times 10^{10}$ , 100  $\mu$ g BEC-EVs), and BMSC-EVs ( $1 \times 10^{10}$ , 100  $\mu$ g BMSCs-EVs). MCAo model establishment was conducted as our previous work described,<sup>37</sup> briefly, incisions were made in rat neck, and rat common carotid artery, internal carotid artery, and external carotid artery were separated, and then, external carotid artery was temporarily ligated, and a monofilament coated with silicone was inserted approximately 1.6–1.8 cm from the micro incision made at rat common carotid artery, via the internal carotid artery and upward to the middle cerebral artery. After modeling, the wounds of rats were sutured and disinfected. Rats were kept warm at 37°C to avoid loss of body temperature by animal heating pad. Food and water were supplied freely in the cage after surgery. The BEC-EVs, BMSC-EVs and DiI labeled EVs were injected by tail vein within 30 minutes after the MCAo procedure, and the rats in MCAo and SHAM groups were injected with PBS. 6 and 24 hours post-surgery, rats were sacrificed by inhalation of carbon dioxide for brain sampling.

## Isolation of Brain Cortex Microvessels

Brain microvessels were isolated as the previous study.<sup>39</sup> Briefly, after rats sacrifice, the whole brains were immersed in MCDB 131 medium (10372019, Gibco). The cortex was roughly separated and homogenated in MCDB 131 medium and the mixture was centrifuged at 2000 g under 4°C for 5 mins. The precipitate was resuspended in 15% dextran (MW ~ 70 kDa; Sigma-Aldrich). After centrifugating at 10,000 g for 15 min under 4 °C, the pellets rich in brain cortex microvessels were obtained for further experiments.

## Evans Blue Dye Leakage for the Measurement of BBB Leakage and TTC Staining

For BBB leakage measurement, rats were injected intravenously with 2% Evans Blue (4 mL/kg) prior to sacrifice and kept circulating for 1 h. After intracardiac perfused with 50 mL PBS under anesthesia, the brains were imaged by IVIS<sup>®</sup> Spectrum small animal image system (PerkinElmer) at 620 nm excitation wavelength and 710 nm emission wavelength. Afterward, equal weighted ischemic brain hemispheres were homogenized with 1 mL 50% trichloroacetic acid, and centrifuged at 15,000 g under 4 °C for 15 min. The supernatant was mixed with 4 times volume of ethanol, and the fluorescence intensity was determined by microplate reader (SpectraMax M5) at 620 nm excitation and 710 nm emission. The Evans Blue concentration was evaluated by using Evans Blue standard curve. For TTC staining, brain samples were cut into 2 mm coronal slices and stained with 2% 2,3,5-Triphenyl tetrazolium chloride (TTC, T819366, Macklin) for 20 minutes at 37 °C in a light-proof environment. Ratio of stained white area (infarct volume) to whole brain area was measured by ImageJ software and calculated according to previous published study.<sup>40</sup> Briefly, the infarct ratio was calculated by using the following equation:  $I=(M-S)/T$ . M is the area of infarct, S is the brain swelling area, and  $S=M-T$ , where M is the area of the ischemic hemisphere slices and T is the area of the non-ischemic hemisphere slices.

## Neurological Function Scores Evaluation

The neurological function scores in rats were assessed using the Longa score (5-points scoring scale)<sup>41</sup> and modified Neurological Severity Score (mNSS) score (18-points scoring scale)<sup>37</sup> at the end of experiments. The experimental scores were recorded by trained technician who was unaware of the experimental design. The detailed scores criteria was attached in [Supplementary File](#).

## Corner and Adhesive Removal Tests

For corner test, the experiments were carried out according to previous study.<sup>42</sup> In short, rats were placed in the middle front of two boards (30 cm×20 cm×1 cm) attached at a 30° angle. After rats entering to the deep part, they reared forward and upward, and then turned back to face the open end. The right turns ratio was recorded in 10 runs of each rats. All rats were trained to adapt to the experiments 3 days before the MCAo modeling. For adhesive removal test, a previous study was referenced with minor modifications.<sup>43</sup> Adhesive tape (3mm×4mm) was applied on the right forepaws of rats, and the time that rats used to remove the tape was recorded (maximum recording time:120 s) to assess the neurological function.

## In-Situ Zymography

In-situ zymography was performed according to previous report with modifications.<sup>44</sup> Briefly, unfixed brain samples were prepared as 20  $\mu\text{m}$  frozen sections, and processed by EnzCheck Gelatinase/Collagenase Assay Kit (E-12055, Invitrogen). Sections were incubated with reaction buffer containing 100  $\mu\text{g}/\text{mL}$  FITC-labeled DQ-gelatin at 37  $^{\circ}\text{C}$  for 2 h. After washed in PBS for 3 times, and fixed by 4% PFA, the sections were observed under fluorescent microscopy (DMI8, Leica). The MMPs activity was determined as green fluorescence intensity calculated by imageJ software.

## Western Blotting

Protein samples were lysed and extracted from cell samples, brain microvessels, and EVs. After denaturation by boiling, the proteins were separated with 10% sodium SDS polyacrylamide gels and transferred to 0.22  $\mu\text{m}$  pore sized polyvinylidene difluoride (PVDF) membranes (1620177, Bio-Rad). Blocked with 5% skimmed milk, the membranes were then incubated with primary and secondary antibodies. ChemiDoc MP Imaging System (Bio-Rad) was used to image the bands, and grey value was calculated by ImageJ software. Antibodies used in the study were provided in [Supplementary File](#).

## Immunofluorescence

After the rats were sacrificed, 50 mL cold PBS and 50 mL cold 4% PFA were intracardiac perfused, and then, the whole brains were collected and further fixed in 4% PFA, and gradient dehydrated in 15% and 30% sucrose solution. 10  $\mu\text{m}$  cryosections were made by a microtome (CryoStar NX70, Thermo Fisher Scientific). For cell samples, BECs were cultured in confocal dish, and followed by OGD and EVs administration. Tissue sections and cells samples were fixed by 4% PFA and permeabilized by 0.1% Triton X-100. After blocking in 5% BSA, primary and secondary antibodies were incubated with cell samples and tissue sections, respectively. Followed by washing, DAPI was stained for nucleus indicating, and lectin (*Lycopersicon Esculentum* (Tomato) Lectin (LEL, TL), DyLight 488, Vector) was stained for vessels visage. Antibodies used in the study were provided in [Supplementary File](#). The slices were imaged by fluorescent microscope (DMI8, Leica) or confocal microscope (SP8, Leica). Mean fluorescence intensity were analyzed by using ImageJ software.

## siRNA Transfection

Caveolin-1 and CD147 siRNAs were synthesized by GenePhrama (GenePhrama, Shanghai) and were transfected in BECs by using lipofectamine 2000 reagent (11668027, Invitrogen) according to the manufacturer's protocol. Protein samples were collected 72 h after transfection. siRNA sequences were provided in [Supplementary File](#).

## Real-Time Reverse Transcriptase-Polymerase Chain Reaction (RT-PCR)

BECs total RNA was extracted by Trizol reagent (15596018, Invitrogen) and reverse transcribed to cDNA by using qPCR RT kit with gDNA remover (MF949-01, Mei5bio). RT-PCR was conducted by using primers and SYBRgreen M5 HiPer Realtime PCR mix (MF015-01, Mei5bio) in QuantStudio™ 7 Flex Real-Time PCR System (Thermo Fisher Scientific). Relative mRNA expression level was calculated by the comparative  $2^{-\Delta\Delta\text{Ct}}$  method.

Primers used in this study were provided in [Supplementary File](#).

## Statistical Analysis

All experimental data were presented as mean  $\pm$  standard deviation (SD) analyzed by using GraphPad Prism 8 software. Significant differences were determined by one-way analysis of variance (ANOVA) followed by Tukey's multiple comparisons test, when P value  $<0.05$ , the statistical significance was determined. All data were normalized and were presented as fold of control or sham groups.

## Results

### The Size, Morphology, and Cellular Internalization of EVs

To purify EVs from BECs and BMSCs, we collected cells culture medium and combined the commercial Exo-Prep exosome isolation kits with ultracentrifugation technologies, and the brief protocol as the scheme showed in (Figure 1A). Next, we evaluated the nanoparticle size of the isolated EVs and confirmed the average size of BMSC-EVs was around 183 nm, and BEC-EVs was 184 nm, respectively (Figure 1B). Based on the nanosize analysis, most EVs are sized approximately 50–250nm, which is the typical size of sEVs or exosomes (Figure 1C). Subsequently, the typical EVs markers ALIX, TSG101, CD9, and CD63 were expressed in two kinds of EVs, whereas the endoplasmic reticulum marker Calnexin was highly expressed in BECs and BMSCs, and was nearly absent in EVs and the supernatants after EVs isolation (Figure 1D). To determine the morphology of EVs, TEM images showed that two kinds of isolated EVs had a intact spherical shape (Figure 1E). Furthermore, to verify whether BEC-EVs and BMSC-EVs can be phagocytized by BECs, we labeled two kinds of EVs by DiI, and co-cultured DiI-EVs with BECs, and as expected, both of them were internalized by BECs (Figure 1F). Altogether, the above results demonstrated that our isolated EVs was pure, and preserved the ability to be uptake by BECs.

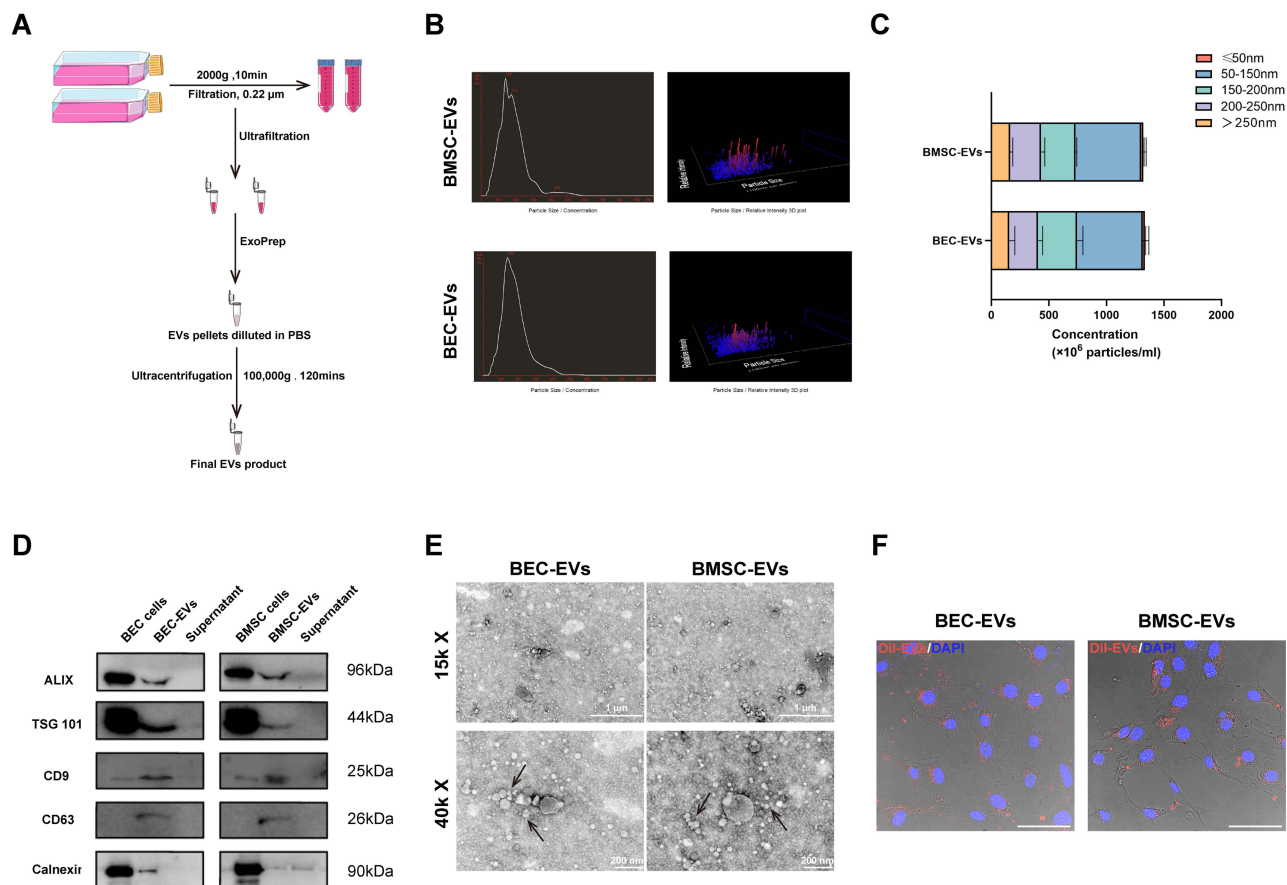


**Figure 1** Characterization of BEC-EVs and BMSC-EVs. **(A)** Schematic diagram of EVs isolation and purification. **(B)** NTA of BMSC-EVs and BEC-EVs to determine the nanoparticle average size. **(C)** BEC-EVs and BMSC-EVs nanoparticles size distribution based on size evaluated by NTA (n=3). **(D)** EVs markers determination by Western blotting. ALIX, TSG101, CD9, and CD63 were regarded as EVs markers. Calnexin was regarded as cells marker, which was absent in EVs, and supernatant after EVs isolation was used as EVs negative control. **(E)** TEM images of BEC-EVs and BMSC-EVs. Typical EVs were identified by black arrow. The magnification of the upper panel: 15,000 X, scale bar: 1 μm, and the magnification of the lower panel: 40,000 X, scale bar: 200 nm. **(F)** DiI labeled BEC-EVs and BMSC-EVs phagocytosis by BECs. Images were taken when DiI labeled BEC-EVs and BMSC-EVs cultured with BECs for 2h. Scale bar: 50 μm.

## EVs Administration Attenuated the Permeability and MMP Activity in OGD-Insulted BECs

To evaluate the efficacies of BEC and BMSC-EVs administrations on the BECs permeability, we applied OGD-insulted b. End 3 cells co-cultured with two kinds of EVs. The expressions of ZO-1 and Occludin were astonishingly decreased, but they were significantly restored by BEC and BMSC-EVs administrations. And the restorative effect of BMSC-EVs was superior to that of BEC-EVs (Figure 2A and B). In addition, the leakage of BECs monolayer in transwell after OGD stimulation was higher by about 1.5-fold than that in normoxia condition, and it was declined by two kinds of EVs administrations with no difference (Figure 2C). Moreover, the immunofluorescent staining signals of ZO-1 and Occludin in OGD-insulted BECs were attenuated, but significantly recovered by BEC and BMSC-EVs treatments (Figure 2D and E).

Next, we tested the effects of BEC and BMSC-EVs on the expression and activation of MMPs in BECs after OGD stimulation. The expressed levels of MMP-2/9 were obviously upregulated, while downregulated by BEC and BMSC-EVs treatments (Figure 3A and B). Similarly, the mRNA levels of MMP-2/9 were also enhanced by 3–4 folds after OGD stimulation, whereas decreased by two kinds of EVs treatments (Figure 3C). Additionally, we employed gelatin zymography assay to detect the release and activation of MMPs in OGD-insulted BECs culture medium (Figure 3D). Analogously, the activity of MMP-2/9 was promoted, and harnessed by BEC and BMSC-EVs treatments, especially by BMSC-EVs administration (Figure 3E and F).

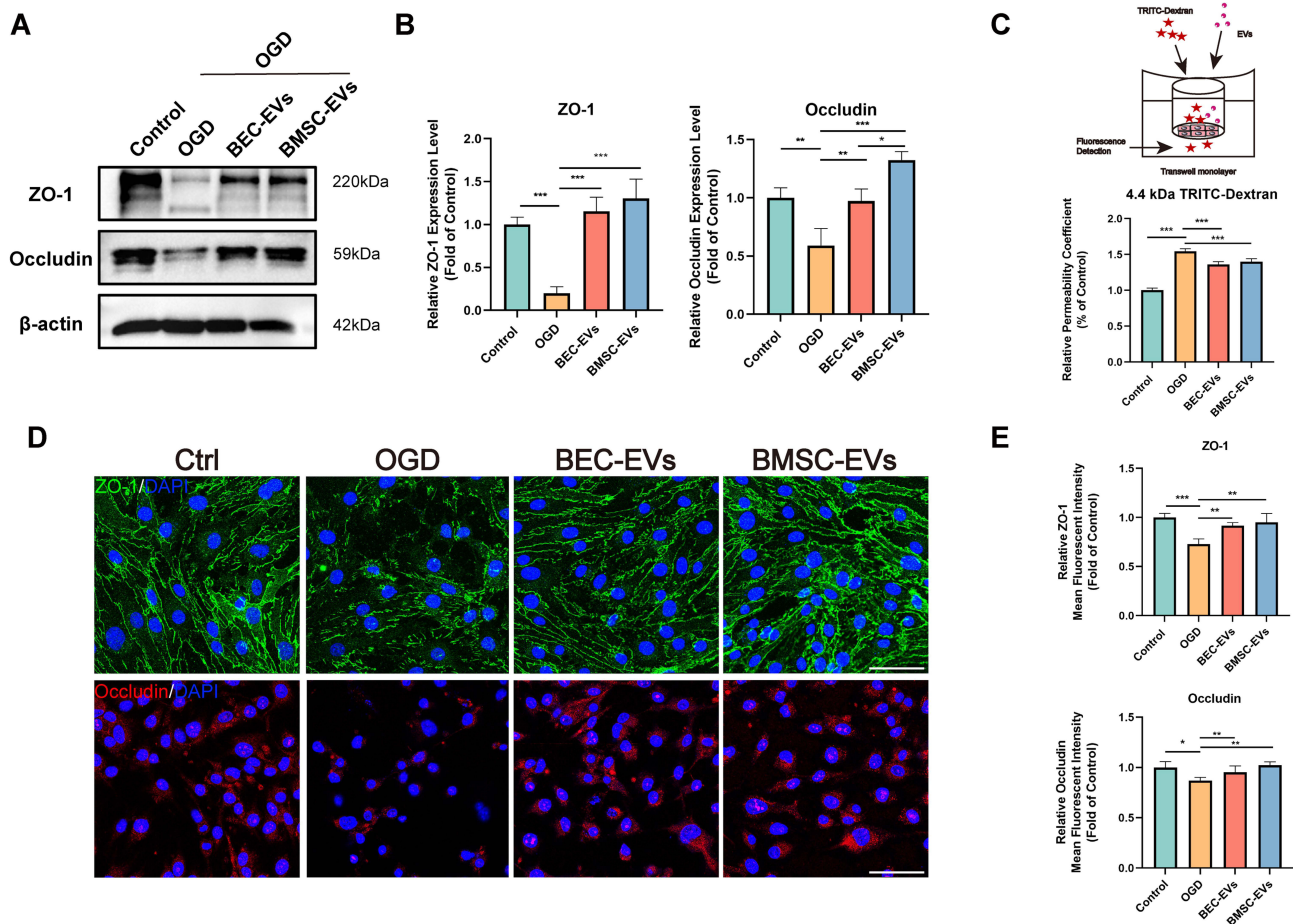


**Figure 2** BEC-EVs and BMC-EVs administrations decreased leakage of BECs and increased TJ proteins expression after OGD. **(A)** Western blotting of ZO-1 and Occludin in OGD-insulted BECs after EVs treatment. **(B)** Relative quantitative analysis of ZO-1 and Occludin (n=3). **(C)** Sketch of transwell assay and the relative OGD-insulted BECs monolayer leakage after EVs treatment (n=4). **(D)** Immunofluorescence staining of ZO-1 and Occludin in OGD-insulted BECs after EVs treatment. Scale bar: 50  $\mu$ m. **(E)** Mean fluorescence intensity relative quantification of ZO-1 and Occludin (n=4). \*\*\* $P < 0.001$ , \*\* $P < 0.01$ , \* $P < 0.05$ .

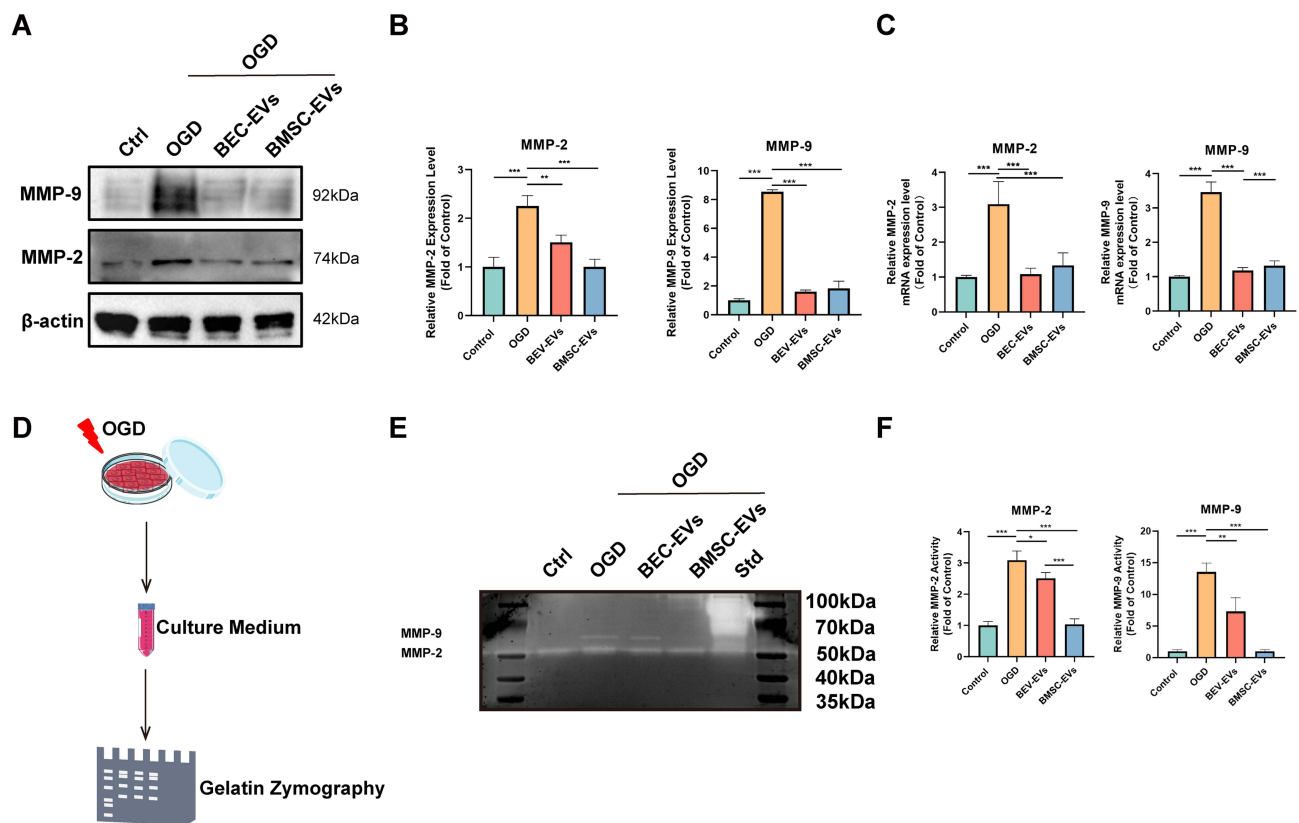


**Figure 3** BEC-EVs and BMC-EVs administrations attenuated MMPs expression and activity in OGD-insulted BECs. **(A)** Western blotting of MMP-2/9 after EVs treatment. **(B)** Relative quantitative analysis of MMP-2/9 ( $n=3$ ). **(C)** Relative quantification of MMP-2/9 mRNA expressed levels by RT-PCR ( $n=3$ ). **(D)** Schematic diagram of MMPs activity. **(E)** MMP-2/9 activity evaluation by gelatin zymography in OGD-insulted BECs culture medium after EVs treatment. Std: positive control of MMP standard sample. **(F)** Relative quantification of MMP-2/9 activity ( $n=3$ ). \*\*\* $P < 0.001$ , \*\* $P < 0.01$ , \* $P < 0.05$ .

Taken together, the above results demonstrated the positive intervention effects of EVs from BECs and BMSCs on the permeability and MMP-2/9 activation in OGD-insulted BECs.

## EVs Administration Alleviated BBB Permeability and Neurological Function Deficit After Cerebral Ischemia in Rats

Thereafter, to determine the BBB protective efficacies of BEC and BMSC-EVs administrations, we established permanent MCAo model in rats, and administrated EVs via tail vein immediately after the rats were modeled. The chart flow of the experiment was presented in (Figure 4A). After 6 hours cerebral ischemia, the DiI labeled EVs were significantly ingested by lectin labeled BECs in brain vessels and Tuj-1 labeled neurons, and the ingestion rate of both kinds of EVs in BECs is higher than that in neurons (Figure 4B). Also, the administrated BEC and BMSC-EVs reduced the brain infarct volume significantly with no difference (Figure 4C).

Additionally, the Evans Blue leakage in ischemic brain hemisphere was significantly reduced by two kinds of EVs administrations, especially by BMSC-EVs treatment (Figure 4D). Notably, the neurological function of MCAo rats evaluated by Longa score, mNSS, corner test and adhesive removal test was significantly improved by two kinds of EVs treatments after 24 hours cerebral ischemia (Figure 4E–H). The results proved that the intravenous administrated BEC and BMSC-EVs contributed to the maintenance of BBB integrity and neurological outcome improvement after acute cerebral ischemia in rats.

## EVs Administration Enhanced the Expression of TJ Proteins and Suppressed the Activity of MMPs in MCAo Rats

The result of Western blotting showed ZO-1 expression in brain microvessels from ischemic cortex was enhanced by both kinds of EVs administrations; however, Occludin expression was only increased by BMSC-EVs administration

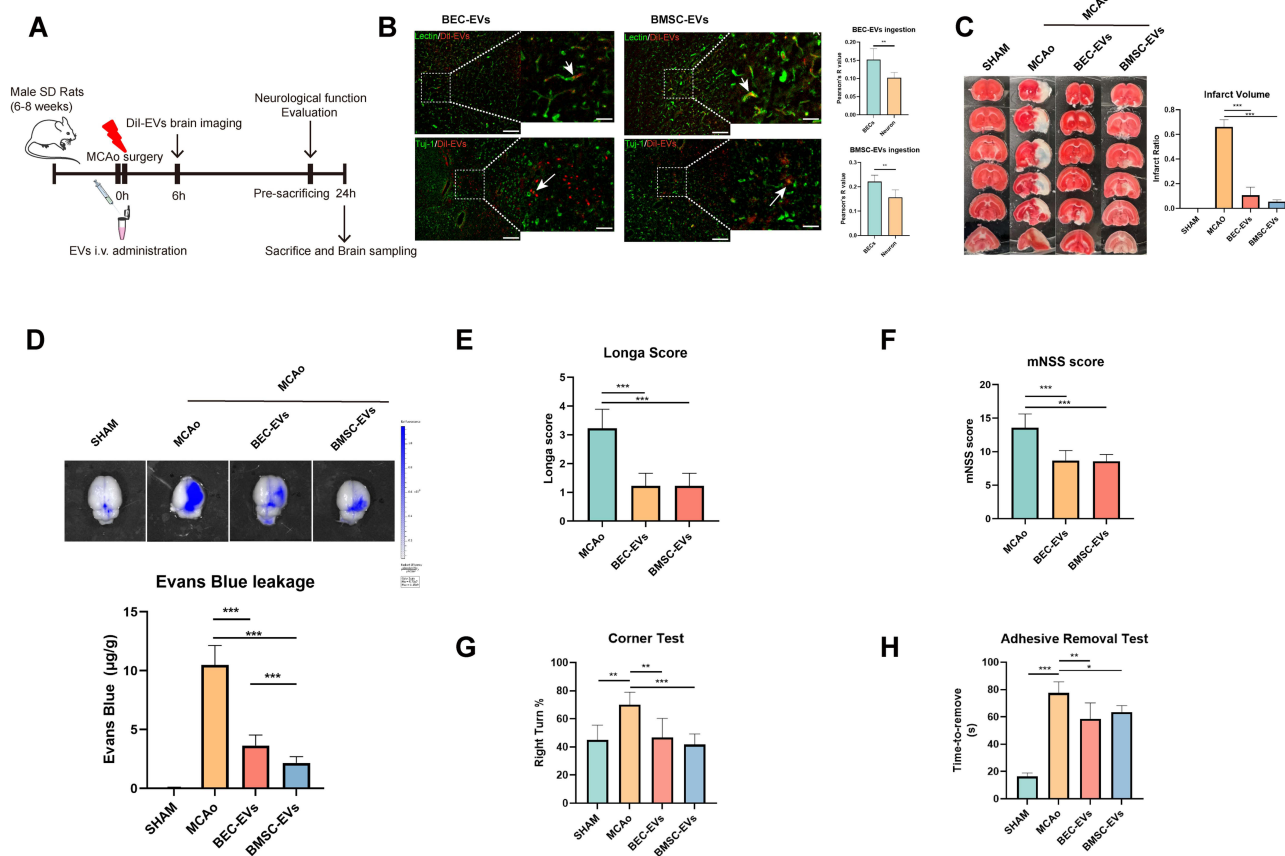


**Figure 4** BEC-EVs and BMC-EVs administrations reduced BBB leakage and ameliorated neurological function in MCAo rats. **(A)** Schematic diagram of animal experimental procedure in MCAo rats. **(B)** Dil labeled BEC-EVs and BMSC-EVs were internalized by brain endothelial cells and neurons. Lectin was regarded as endothelial marker, and Tuj-1 was recognized as neurons marker. Original image Scale Bar: 200 µm. Enlarged image Scale Bar: 50 µm. **(C)** TTC staining of rat brain sections after EVs treatment, and relative quantification of brain infarct size (n=4). **(D)** Upper panel: Evans Blue brain leakage after EVs administration. Lower panel: Evans Blue leakage quantification (n=9). **(E)** Neurological function evaluation by Longa score (n=10). **(F)** Neurological function evaluation by mNSS score after EVs administration in MCAo rats (n=10). **(G)** Neurological function evaluation by corner test (n=6). **(H)** Neurological function evaluation by adhesive removal test (n=6). \*\*\* $P < 0.001$ , \*\* $P < 0.01$ , \* $P < 0.05$ .

(Figure 5A). Interestingly, the immunofluorescence staining results had similar trend (Figure 5B and C). Afterward, the in-situ zymography results showed that the MMPs activity in ischemic brain was dramatically upregulated and attenuated by two kinds of EVs administrations (Figure 5D and E). Although the quantitative analysis indicated MMPs activity in BMSC-EVs group was lower than that in BEC-EVs group, there was no statistic difference between these two groups. The ameliorated results in TJ proteins and MMPs activity in MCAo rats were consisted with those in OGD-insulted BECs after EVs treatment.

## EVs Administration Suppressed Caveolin-1/CD147/VEGF Expressions in MCAo Rats

To further determine the mechanism of EVs on the maintenance of BBB integrity, we tested the expressions of Caveolin-1, CD147, VEGFR2, and VEGFA in MCAo rats. Western blotting results showed that, the expression levels of Caveolin-1, CD147, VEGFR2 and VEGFA were significantly upregulated in brain microvessels from ischemic cortex. The administration of BMSC-EVs was evidenced in downregulation of all these indicators, whereas for the administration of BEC-EVs, it only downregulated VEGFA, Caveolin-1 and CD147 expressions but CD147 expression in BEC-EVs group had no statistical significance compared with that in MCAo group (Figure 6A and B). The immunofluorescence staining results also presented the Caveolin-1, VEGFR2 and CD147 signals notably declined in BMSC-EVs group, whereas in BEC-EVs group, although the three signals were also attenuated, VEGFR2 signal had no significant difference compared with that in MCAo group (Figure 6C–F). The above results illustrated the treatments of BEC and BMSC-EVs, especially BMSC-EVs administration played predominant role in the inhibiting Caveolin-1/CD147/VEGFR2 pathway in MCAo rats.

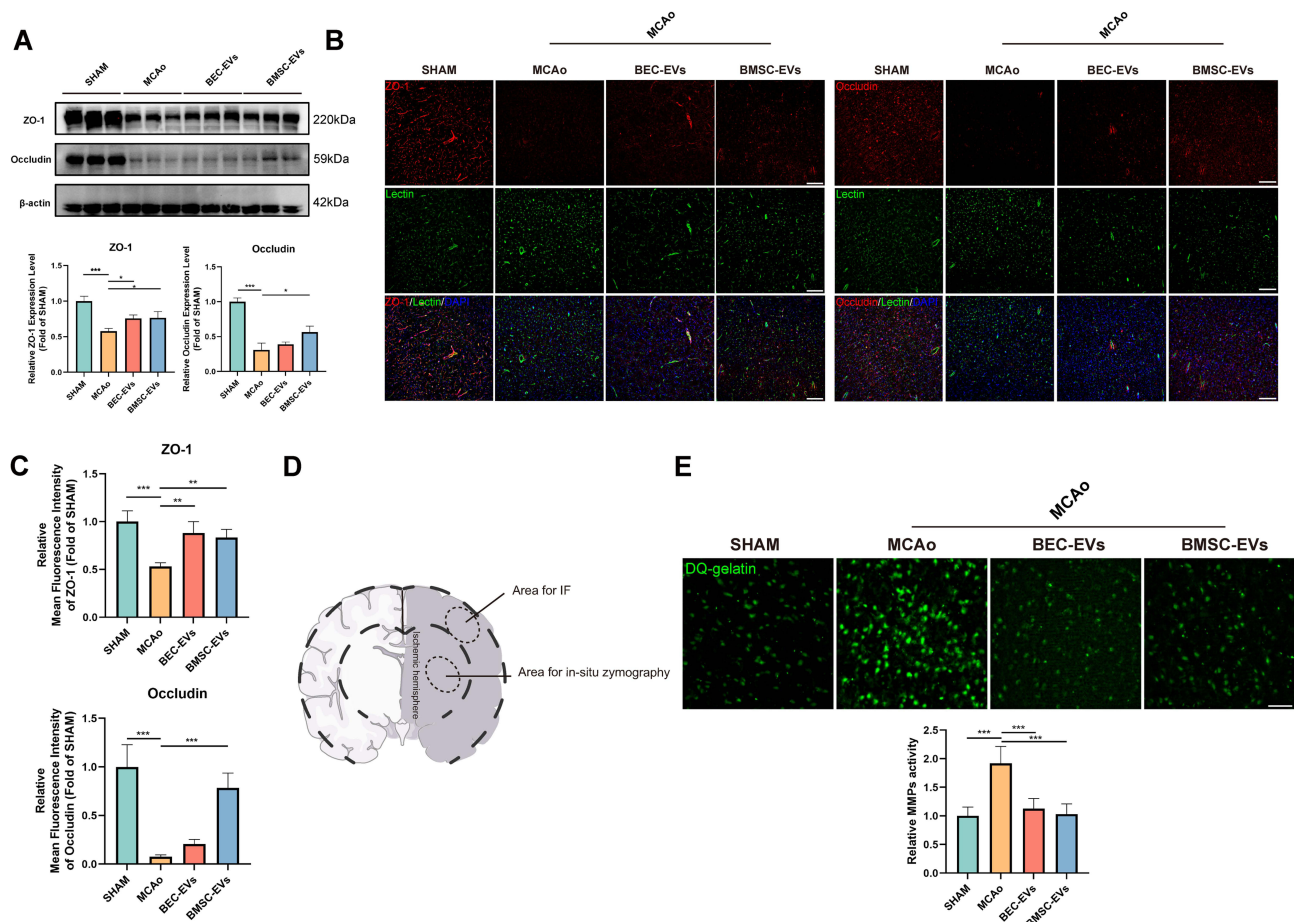


**Figure 5** BEC-EVs and BMSC-EVs administrations enhanced TJ proteins and restrained MMPs activity in MCAo rats. **(A)** Western blotting and relative quantification of ZO-1 and Occludin in brain microvessels after EVs treatment groups (n=3). **(B)** Immunofluorescence staining of ZO-1 and Occludin in ischemic brain cortex. Scale bar: 200  $\mu$ m. **(C)** Relative quantification of mean fluorescence intensity of ZO-1 and Occludin (n=4). **(D)** Schematic diagram of Immunofluorescence observation area and In-situ zymography zone. **(E)** MMPs activity detection and quantitative analysis (n=4). Scale bar: 50  $\mu$ m \*\*\*P < 0.001, \*\*P < 0.01, \*P < 0.05.

## Caveolin-1/CD147/VEGFR2/MMP Pathway is Pivotal in OGD-Insulted BECs Permeability

To better understand the role of Caveolin-1/CD147/VEGFR2/MMP pathway in BBB protection, we employed OGD-insulted BECs to simulate BBB damage after IS. After OGD stimulation, the transwell assay results suggested that the increased BECs monolayer leakage was partly inhibited by the administrations of Cav-1 and CD147 siRNAs (Figure 7A–C), suggesting Cav-1 and CD147 exerted important actions on BECs permeability. Additionally, we also tested the MMPs activity by gelatine zymography. As expected, the knockdown of Caveolin-1 and CD147 by siRNAs abolished the activation of MMP-2/9 in OGD-insulted BECs (Figure 7D). Thereafter, we further investigated the relationships among Caveolin-1, CD147, VEGFR2 and VEGFA. It showed that OGD induced the upregulation of CD147, VEGFR2 and VEGFA expressions was partly muted by Cav-1 siRNA, indicating CD147, VEGFR2 and VEGFA were downstream of Caveolin-1 (Figure 7E and F). Similarly, we observed a significant decline of VEGFR2 and VEGFA expressions and a rise of ZO-1 and Occludin expressions, but no significant alteration for Caveolin-1 expression after CD147 siRNA administration (Figure 7G and H), which further proved that VEGFR2/VEGFA was a downstream of CD147 whereas Caveolin-1 was the upstream. In the above results, our designed two siRNAs for Caveolin-1 and CD147 showed equal knockdown effects and downstream pathways interventions with no significant difference and off-target effect. The above results verified that CD147 had the ability to regulate TJ proteins expression, and Caveolin-1/CD147/VEGFR2/MMP pathway had a dominant effect on OGD-insulted BECs permeability.

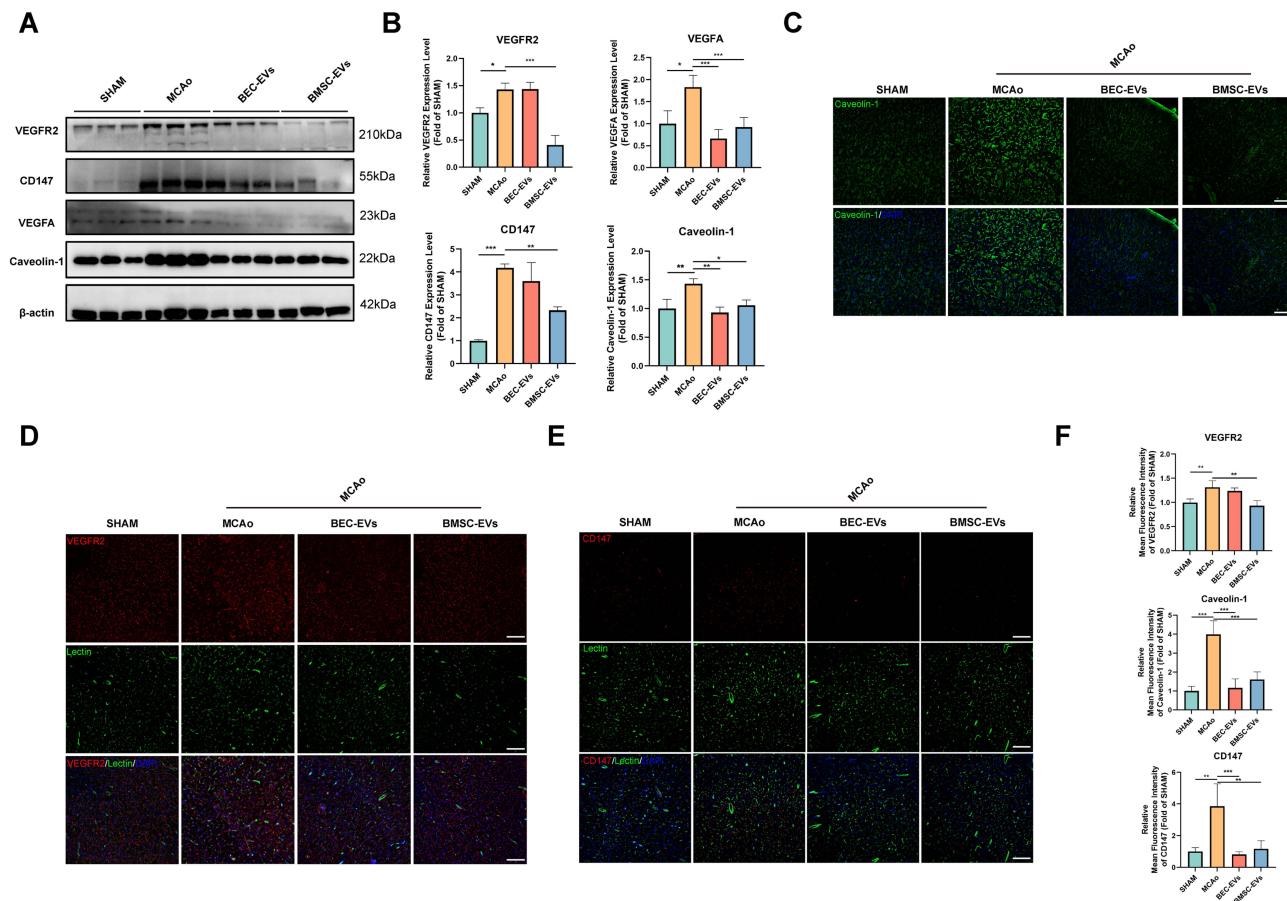


**Figure 6** BEC-EVs and BMSC-EVs administrations inhibited Caveolin-1/CD147/VEGFR2 pathway in MCAo rats. (A) Western blotting of CD147, VEGFR2, VEGFA, and Caveolin-1 in brain microvessels. (B) Relative quantification of CD147, VEGFR2, VEGFA, and Caveolin-1 in brain microvessels (n=3). (C–E) Immunofluorescence staining of Caveolin-1, CD147, VEGFR2 in ischemic brain cortex. Scale bar: 200  $\mu$ m. (F) Relative quantification of mean fluorescence intensity of Caveolin-1, CD147 and VEGFR2 (n=4). \*\*\* $P < 0.001$ , \*\* $P < 0.01$ , \* $P < 0.05$ .

## Discussion

In the present study, our results demonstrated the therapeutic efficacies of BEC and BMSC-EVs on the maintenance of BBB integrity after IS. It showed that the administrations of BEC and BMSC-EVs significantly enhanced the expressions of ZO-1 and Occludin, inhibited BBB leakage, and harnessed the activation of MMP-2/9, which was related to the suppression of Caveolin-1/CD147/VEGFR2/MMP pathway.

EVs are believed to be “nano sized messenger” which convey complex biological substances such as non-coding RNA and biofunctional proteins to mediate cells communication.<sup>45</sup> EVs are easy to cross BBB, with fewer concerns of immunogenicity, microvascular occlusion, and uncontrolled proliferation than their parent cells.<sup>46</sup> Accordingly, EVs from apposite cell sources might be promising candidate for IS treatment. In stroke treatment, dozens of studies have illustrated that the administration of EVs can ameliorate pathologic outcomes on neurovascular unit (NVU) injury.<sup>47</sup> Especially EVs from mesenchymal stem cells, remarkably improved neurological function deficit, BBB disruption, and inflammation activation.<sup>14</sup> For instance, neural stem cells (NPCs) derived EVs can mediate neuronal survival, neuroinflammation response and functional recovery in rat MCAo model.<sup>48</sup> Mesenchymal stem cells derived EVs also proved to promote angiogenesis after IS in rats.<sup>49</sup> And adipose stem cells derived EVs were reported to transfer miR-25 for autophagy inhibition in MCAo model, which enhanced the neurological outcomes. Apart from stem cells, BECs derived EVs were also reported to induce neuroprotective effects by miR-126 dependent pathway in diabetic stroke mice model,<sup>50</sup> and endothelial progenitor cells derived EVs were proved optimal to treat MCAo induced stroke mice when combined with NPCs derived EVs.<sup>51</sup> So, different stem cells and endothelial cells originated EVs are of great significance for IS therapeutic strategy.

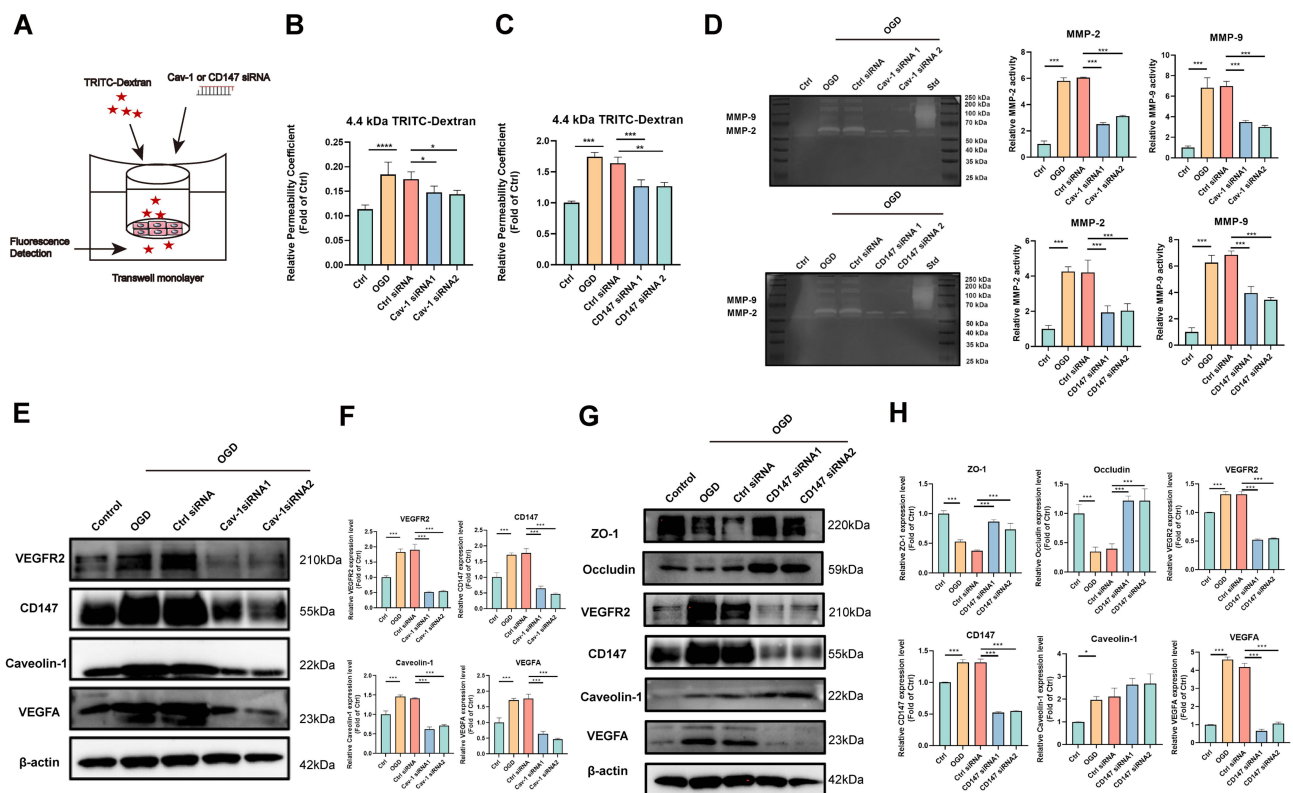


**Figure 7** Caveolin-1/CD147/VEGFR2/MMP pathway played predominant role in the permeability of OGD-insulted BECs (A) Sketch of transwell assay in OGD-insulted BECs and the transfection of Caveolin-1 and CD147 siRNA. (B) Relative leakage OGD-insulted BECs monolayer after Caveolin-1 siRNA transfection (n=4). (C) Relative leakage OGD-insulted BECs monolayer after CD147 siRNA transfection (n=4). (D) Caveolin-1 and CD147 siRNA reduced MMP-2/9 activity evaluated by gelatin zymography in OGD-insulted BECs and relative quantification. Std: positive control of MMP standard sample. (E and F) Western blotting of CD147, Caveolin-1, VEGFR2, and VEGFA in OGD-insulted BECs after Caveolin-1 siRNA transfection and relative quantification (n=3). (G and H) Western blotting of ZO-1, Occludin, CD147, VEGFR2, Caveolin-1, and VEGFA in OGD-insulted BECs after CD147 siRNA transfection and relative quantification (n=3). \*\*\* $P < 0.001$ , \*\* $P < 0.01$ , \* $P < 0.05$ .

Our previous study demonstrated BEC and BMSC-EVs administrations effectively alleviated BBB damage in MCAO rats, and the potential mechanisms are partly related to the inhibition of Caveolin-1 dependent ZO-1 and Claudin-5 endocytosis.<sup>37</sup> Apart from the TJ proteins endocytosis, the broader therapeutic mechanisms of EVs from BECs and BMSCs should be defined.

MMPs are a series of calcium-dependent zinc endopeptidases and have been broadly reported to deteriorate BBB integrity after IS.<sup>52</sup> Among MMPs category, the activation of MMP-2/9 is mainly responsible for the degradation of ECM, and TJ proteins injury, neuroinflammation, brain edema and cerebral hemorrhage transformation in acute IS.<sup>23,53</sup> Inhibition of MMP-2/9 by gene silencing or inhibitors is effective to improve post-stroke outcomes.<sup>24</sup> For example, applying gelatinase inhibitor SB-3CT to inhibit the activity of MMPs contributed to the function recovery of NVU in mice embolic IS.<sup>54</sup> However, the exact mechanisms of how NVU components produce and activate MMPs fails to be fully understood. In recent years, CD147 is newly identified as MMPs upstream, and the glycosylation of CD147 is crucial for MMPs activation.<sup>22</sup> Some membrane proteins can bind to CD147 and regulate its glycosylation, and Caveolin-1 is regarded as one of the proteins that can actively participate in the high-glycosylation of CD147.<sup>22,55</sup> Our previous study evidenced that the upregulation of Caveolin-1 involved in the endocytosis of TJ proteins after IS resulted in BBB disruption and neurological function exacerbation in MCAO rats.<sup>37</sup> Studies have illustrated that Caveolin-1 can bind to low glycosylated CD147 and inhibit its high-glycosylation, which further reduced MMPs induction.<sup>55,56</sup> Nevertheless, the role of Caveolin-1 binding to CD147 to increase MMPs activity against BBB integrity is still ambiguous after cerebral ischemia. In diabetic MCAO rat model, Caveolin-1 was proved to be linked with high glycosylated CD147 in BECs and astrocytes, which activated MMP2/9 to degrade BBB components after r-tPA treatment.<sup>36</sup> Though the glycosylation of CD147 was reported to induce MMPs activation, its exact downstream mechanism is unclear. VEGF

and its receptors are classic angiogenesis mediators. However, their increased expressions after stroke were able to enhance BBB permeability.<sup>5</sup> Evidence showed that VEGF was a downstream of CD147, and the decreasing of CD147 was proved to dwindle VEGF production in endothelial cells.<sup>31</sup> Regrettably, few studies reported crosstalk between CD147 and VEGF in stroke study. Additionally, Caveolin-1 involved in the regulation of VEGF and MMPs activities in BECs had been definite, because genetic knockdown of Caveolin-1 decreased MMPs activity and VEGF-dependent angiogenesis in human endothelial cells,<sup>57</sup> and identically, knockdown of Caveolin-1 by siRNA was verified to inhibit the expression of MMP-9 in BECs after tPA treatment.<sup>58</sup> The above results trigger us to focus on the relationship between Caveolin-1/CD147/VEGFR2/MMP pathway and BBB integrity after IS.

In our study, we used siRNA to knockdown CD147 and Caveolin-1, respectively, and found the BECs leakage and the activity of MMPs significantly declined after OGD stimulation. Simultaneously, low expressions of CD147, VEGFR2 and VEGFA were regarded as Cav-1 downregulation by the administration of Cav-1 siRNA; the knockdown of CD147 by siRNA transfection decreased the expressions of VEGFA and VEGFR2, as well as recovered the expressions of ZO-1 and Occludin, however the CD147 knockdown did not change the Caveolin-1 expression. The results evidenced that Caveolin-1 was upstream of CD147/VEGFR2/MMP pathway, and the pathway suppression contributed to the attenuation of BBB permeability.

Our results also showed that BMSC-EVs administration was more evidenced in downregulating CD147 and VEGFR2 expression and inhibiting MMP2 activity, together with enhancing Occludin expression in brain microvessels from ischemic cortex, which definitely explained the phenomenon why BBB leakage in BMSC-EVs group was significantly lower than that in BEC-EVs group in MCAo rats. As BMSC-EVs were widely demonstrated to mediate NVU recovery via different pathways,<sup>14</sup> and our study also demonstrated BMSC-EVs were superior to BEC-EVs in the maintenance of BBB integrity in MCAo rats. Therefore, BMSC-EVs treatment ought to be more promising therapy for acute IS.

The current study remains some limitations, first, our permanent MCAo rat model is very suitable for simulating acute large vessel occlusion in clinical stroke practice; however, the model is not optimal for ischemic-reperfusion study, and subsequent studies should discover the EVs therapeutic effects on transient MCAo models for better understanding of EVs role in ischemic-reperfusion injury. Second, our EVs isolating and purification presented low EVs production and recovery rates, though currently, there is no economic and perfect measures for EVs high output isolation,<sup>59</sup> this limitation may hinder the EVs widely clinical translation. On the other hand, the limited understanding of EVs content and their complex treatment mechanisms may also be obstacles for EVs application in clinic. More studies toward EVs biochemistry content and their border mechanisms are essential for EVs research development. Upliftingly, based on records in clinicaltrials.gov, many EVs clinical trials have been carried out for stroke treatments (eg NCT03384433, NCT06138210, and NCT05326724), through which, EVs therapeutic may finally benefit stroke patients in the future, and advance the development of stroke interventions.

## Conclusion

In conclusion, our study firstly affirmed the therapeutic efficacies of BEC-EVs and BMSC-EVs on the maintenance BBB integrity and neurological outcome after IS, and the mechanisms are partly related to inhibiting Caveolin-1/CD147/VEGFR2/MMP pathway. Integrately, the employment of BMSC-EVs is regarded as more promising treatment strategy.

## Data Sharing Statement

All datasets that support the study are available from the corresponding author on reasonable request.

## Ethics Approval

All animal experiments were approved and supervised by the Ethics Committee of the University of Macau. Animal welfare was ensured according to the Guide for the Care and Use of Laboratory Animals.

## Acknowledgments

We thank Faculty of Health Sciences of University of Macau for their animal offering in this work. Additionally, we thank Fan Zhang for drawing work of graphic abstract, and we appreciate group members from Dr. Jiahong LU and Dr. Ying Zheng's group for their kind technical assistance.

## Funding

This work is funded by the University of Macau (MYRG2022-00221-ICMS, MYRG-CRG2022-00011-ICMS), Guangdong Natural Science Fund (General Programme, no. 2023A1515010034), and the National Natural Science Foundation of China (NSFC No. 82074051).

## Disclosure

The authors declare no competing interests in this work.

## References

1. Popa-Wagner A, Petcu EB, Capitanescu B, Hermann DM, Radu E, Gresita A. Ageing as a risk factor for cerebral ischemia: underlying mechanisms and therapy in animal models and in the clinic. *Mech Ageing Dev.* 2020;190:111312. doi:10.1016/j.mad.2020.111312
2. Yousufuddin M, Young N. Aging and ischemic stroke. *Ageing.* 2019;11(9):2542–2544. doi:10.18632/aging.101931
3. Virani SS, Alonso A, Benjamin EJ, et al. Heart disease and stroke statistics-2020 update: a report from the American Heart Association. *Circulation.* 2020;141(9):e139–e596. doi:10.1161/cir.0000000000000757
4. Yang Y, Rosenberg GA. Blood-brain barrier breakdown in acute and chronic cerebrovascular disease. *Stroke.* 2011;42(11):3323–3328. doi:10.1161/strokeaha.110.608257
5. Jiang X, Andjelkovic AV, Zhu L, et al. Blood-brain barrier dysfunction and recovery after ischemic stroke. *Prog Neurobiol.* 2018;163–164:144–171. doi:10.1016/j.pneurobio.2017.10.001
6. Chamorro Á, Dirnagl U, Urra X, Planas AM. Neuroprotection in acute stroke: targeting excitotoxicity, oxidative and nitrosative stress, and inflammation. *Lancet Neurol.* 2016;15(8):869–881. doi:10.1016/s1474-4422(16)
7. Shi L, Rocha M, Leak RK, et al. A new era for stroke therapy: integrating neurovascular protection with optimal reperfusion. *J Cereb Blood Flow Metab.* 2018;38(12):2073–2091. doi:10.1177/0271678x18798162
8. Zivin JA. Acute stroke therapy with tissue plasminogen activator (tPA) since it was approved by the U.S. Food and Drug Administration (FDA). *Ann Neurol.* 2009;66(1):6–10. doi:10.1002/ana.21750
9. Reeves MJ, Arora S, Broderick JP, et al. Acute stroke care in the US: results from 4 pilot prototypes of the Paul Coverdell National Acute Stroke Registry. *Stroke.* 2005;36(6):1232–1240. doi:10.1161/01.STR.0000165902.18021.5b
10. Joo H, Wang G, George MG. Use of intravenous tissue plasminogen activator and hospital costs for patients with acute ischaemic stroke aged 18–64 years in the USA. *Stroke Vasc Neurol.* 2016;1(1):8–15. doi:10.1136/svn-2015-000002
11. Kawabori M, Shichinohe H, Kuroda S, Houkin K. Clinical trials of stem cell therapy for cerebral ischemic stroke. *Int J Mol Sci.* 2020;21(19):7380. doi:10.3390/ijms21197380
12. Herberts CA, Kwa MS, Hermesen HP. Risk factors in the development of stem cell therapy. *J Transl Med.* 2011;9(1):29. doi:10.1186/1479-5876-9-29
13. Eleuteri S, Fierabracci A. Insights into the secretome of mesenchymal stem cells and its potential applications. *Int J Mol Sci.* 2019;20(18). doi:10.3390/ijms20184597
14. Rahmani A, Saleki K, Javanmehr N, Khodaparast J, Saadat P, Nouri HR. Mesenchymal stem cell-derived extracellular vesicle-based therapies protect against coupled degeneration of the central nervous and vascular systems in stroke. *Ageing Res Rev.* 2020;62:101106. doi:10.1016/j.arr.2020.101106
15. van Niel G, D'Angelo G, Raposo G. Shedding light on the cell biology of extracellular vesicles. *Nat Rev Mol Cell Biol.* 2018;19(4):213–228. doi:10.1038/nrm.2017.125
16. Saint-Pol J, Gosselet F, Duban-Deweer S, Pottiez G, Karamanos Y. Targeting and crossing the blood-brain barrier with extracellular vesicles. *Cells.* 2020;9(4). doi:10.3390/cells9040851
17. Rufino-Ramos D, Albuquerque PR, Carmona V, Perfeito R, Nobre RJ, Pereira de Almeida L. Extracellular vesicles: novel promising delivery systems for therapy of brain diseases. *J Control Release.* 2017;262:247–258. doi:10.1016/j.jconrel.2017.07.001
18. Chen J, Chopp M. Exosome therapy for stroke. *Stroke.* 2018;49(5):1083–1090. doi:10.1161/STROKEAHA.117.018292
19. Li Y, Liu B, Chen Y, et al. Extracellular vesicle application as a novel therapeutic strategy for ischemic stroke. *Transl Stroke Res.* 2021. doi:10.1007/s12975-021-00915-3
20. Venkat P, Chen J, Chopp M. Exosome-mediated amplification of endogenous brain repair mechanisms and brain and systemic organ interaction in modulating neurological outcome after stroke. *J Cereb Blood Flow Metab.* 2018;38(12):2165–2178. doi:10.1177/0271678x18782789
21. Xin W, Qin Y, Lei P, Zhang J, Yang X, Wang Z. From cerebral ischemia towards myocardial, renal, and hepatic ischemia: exosomal miRNAs as a general concept of intercellular communication in ischemia-reperfusion injury. *Mol Ther Nucleic Acids.* 2022;29:900–922. doi:10.1016/j.omtn.2022.08.032
22. Grass GD, Toole BP. How, with whom and when: an overview of CD147-mediated regulatory networks influencing matrix metalloproteinase activity. *Biosci Rep.* 2015;36(1):e00283. doi:10.1042/BSR20150256
23. Rempé RG, Hartz AMS, Bauer B. Matrix metalloproteinases in the brain and blood-brain barrier: versatile breakers and makers. *J Cereb Blood Flow Metab.* 2016;36(9):1481–1507. doi:10.1177/0271678x16655551

24. Chaturvedi M, Kaczmarek L. MMP-9 inhibition: a therapeutic strategy in ischemic stroke. *Mol Neurobiol.* 2014;49(1):563–573. doi:10.1007/s12035-013-8538-z
25. Patrizz A, Doran SJ, Chauhan A, et al. EMMPRIN/CD147 plays a detrimental role in clinical and experimental ischemic stroke. *Aging.* 2020;12(6):5121–5139. doi:10.18632/aging.102935
26. Guo H, Li R, Zucker S, Toole BP. EMMPRIN (CD147), an inducer of matrix metalloproteinase synthesis, also binds interstitial collagenase to the tumor cell surface. *Cancer Res.* 2000;60(4):888–891.
27. Sun J, Hemler ME. Regulation of MMP-1 and MMP-2 production through CD147/extracellular matrix metalloproteinase inducer interactions. *Cancer Res.* 2001;61(5):2276–2281.
28. Liu Y, Qi L, Li Z, Yong VW, Xue M. Crosstalk between matrix metalloproteinases and their inducer EMMPRIN/CD147: a promising therapeutic target for intracerebral hemorrhage. *Transl Stroke Res.* 2023. doi:10.1007/s12975-023-01225-6
29. Liu S, Jin R, Xiao AY, Zhong W, Li G. Inhibition of CD147 improves oligodendrogenesis and promotes white matter integrity and functional recovery in mice after ischemic stroke. *Brain Behav Immun.* 2019;82:13–24. doi:10.1016/j.bbi.2019.07.027
30. Jin R, Xiao AY, Chen R, Granger DN, Li G. Inhibition of CD147 (Cluster of Differentiation 147) ameliorates acute ischemic stroke in mice by reducing thromboinflammation. *Stroke.* 2017;48(12):3356–3365. doi:10.1161/strokeaha.117.018839
31. Bougateg F, Quemener C, Kellouche S, et al. EMMPRIN promotes angiogenesis through hypoxia-inducible factor-2 $\alpha$ -mediated regulation of soluble VEGF isoforms and their receptor VEGFR-2. *Blood.* 2009;114(27):5547–5556. doi:10.1182/blood-2009-04-217380
32. Zong J, Li Y, Du D, Liu Y, Yin Y. CD147 induces up-regulation of vascular endothelial growth factor in U937-derived foam cells through PI3K/AKT pathway. *Arch Biochem Biophys.* 2016;609:31–38. doi:10.1016/j.abb.2016.09.001
33. Jickling GC, Liu D, Stamova B, et al. Hemorrhagic transformation after ischemic stroke in animals and humans. *J Cereb Blood Flow Metab.* 2014;34(2):185–199. doi:10.1038/jcbfm.2013.203
34. Won S, Lee JH, Wali B, Stein DG, Sayeed I. Progesterone attenuates hemorrhagic transformation after delayed tPA treatment in an experimental model of stroke in rats: involvement of the VEGF-MMP pathway. *J Cereb Blood Flow Metab.* 2014;34(1):72–80. doi:10.1038/jcbfm.2013.163
35. Huang Q, Zhong W, Hu Z, Tang X. A review of the role of cav-1 in neuropathology and neural recovery after ischemic stroke. *J Neuroinflammation.* 2018;15(1):348. doi:10.1186/s12974-018-1387-y
36. Xie Y, Wang Y, Ding H, et al. Highly glycosylated CD147 promotes hemorrhagic transformation after rt-PA treatment in diabetes: a novel therapeutic target? *J Neuroinflammation.* 2019;16(1):72. doi:10.1186/s12974-019-1460-1
37. Li Y, Liu B, Zhao T, et al. Comparative study of extracellular vesicles derived from mesenchymal stem cells and brain endothelial cells attenuating blood-brain barrier permeability via regulating Caveolin-1-dependent ZO-1 and Claudin-5 endocytosis in acute ischemic stroke. *J Nanobiotechnol.* 2023;21(1):70. doi:10.1186/s12951-023-01828-z
38. McMillin MA, Frampton GA, Seiwel AP, Patel NS, Jacobs AN, DeMorrow S. TGF $\beta$ 1 exacerbates blood-brain barrier permeability in a mouse model of hepatic encephalopathy via upregulation of MMP9 and downregulation of claudin-5. *Lab Invest.* 2015;95(8):903–913. doi:10.1038/labinvest.2015.70
39. Lee YK, Uchida H, Smith H, Ito A, Sanchez T. The isolation and molecular characterization of cerebral microvessels. *Nat Protoc.* 2019;14(11):3059–3081. doi:10.1038/s41596-019-0212-0
40. Kim GS, Yang L, Zhang G, et al. Critical role of sphingosine-1-phosphate receptor-2 in the disruption of cerebrovascular integrity in experimental stroke. *Nat Commun.* 2015;6:7893. doi:10.1038/ncomms8893
41. Cao Y, Sun N, Yang JW, et al. Does acupuncture ameliorate motor impairment after stroke? An assessment using the CatWalk gait system. *Neurochem Int.* 2017;107:198–203. doi:10.1016/j.neuint.2016.10.014
42. Zhang L, Schallert T, Zhang ZG, et al. A test for detecting long-term sensorimotor dysfunction in the mouse after focal cerebral ischemia. *J Neurosci Methods.* 2002;117(2):207–214. doi:10.1016/s0165-0270(02)00114-0
43. Baek H, Park KJ, Kim MJ, Youn I, Kim H. Modulation of cerebellar cortical plasticity using low-intensity focused ultrasound for poststroke sensorimotor function recovery. *Neurorehabil Neural Repair.* 2018;32(9):777–787. doi:10.1177/1545968318790022
44. Liu J, Jin X, Liu KJ, Liu W. Matrix metalloproteinase-2-mediated occludin degradation and caveolin-1-mediated claudin-5 redistribution contribute to blood-brain barrier damage in early ischemic stroke stage. *J Neurosci.* 2012;32(9):3044–3057. doi:10.1523/jneurosci.6409-11.2012
45. Kalluri R, LeBleu VS. The biology, function, and biomedical applications of exosomes. *Science.* 2020;367(6478):eaau6977. doi:10.1126/science.aau6977
46. Boltze J, Arnold A, Walczak P, Jolkonen J, Cui L, Wagner DC. The dark side of the force - constraints and complications of cell therapies for stroke. *Front Neurol.* 2015;6:155. doi:10.3389/fneur.2015.00155
47. Zhang ZG, Buller B, Chopp M. Exosomes - beyond stem cells for restorative therapy in stroke and neurological injury. *Nat Rev Neurol.* 2019;15(4):193–203. doi:10.1038/s41582-018-0126-4
48. Mahdavi-pour M, Hassanzadeh G, Seifali E, et al. Effects of neural stem cell-derived extracellular vesicles on neuronal protection and functional recovery in the rat model of middle cerebral artery occlusion. *Cell Biochem Funct.* 2019. doi:10.1002/cbf.3484
49. Xia Y, Ling X, Hu G, et al. Small extracellular vesicles secreted by human iPSC-derived MSC enhance angiogenesis through inhibiting STAT3-dependent autophagy in ischemic stroke. *Stem Cell Res Ther.* 2020;11(1):313. doi:10.1186/s13287-020-01834-0
50. Venkat P, Cui C, Chopp M, et al. MiR-126 mediates brain endothelial cell exosome treatment-induced neurorestorative effects after stroke in type 2 diabetes mellitus mice. *Stroke.* 2019;50(10):2865–2874. doi:10.1161/STROKEAHA.119.025371
51. Xu X, Zhang H, Li J, et al. Combination of EPC-EXs and NPC-EXs with miR-126 and miR-210 overexpression produces better therapeutic effects on ischemic stroke by protecting neurons through the Nox2/ROS and BDNF/TrkB pathways. *Exp Neurol.* 2022;114235. doi:10.1016/j.expneurol.2022.114235
52. Yang C, Hawkins KE, Dore S, Candelario-Jalil E. Neuroinflammatory mechanisms of blood-brain barrier damage in ischemic stroke. *Am J Physiol Cell Physiol.* 2019;316(2):C135–C153. doi:10.1152/ajpcell.00136.2018
53. Zhao BQ, Tejima E, Lo EH. Neurovascular proteases in brain injury, hemorrhage and remodeling after stroke. *Stroke.* 2007;38(2 Suppl):748–752. doi:10.1161/01.STR.0000253500.32979.d1
54. Cui J, Chen S, Zhang C, et al. Inhibition of MMP-9 by a selective gelatinase inhibitor protects neurovasculature from embolic focal cerebral ischemia. *Mol Neurodegener.* 2012;7:21. doi:10.1186/1750-1326-7-21
55. Tang W, Chang SB, Hemler ME. Links between CD147 function, glycosylation, and caveolin-1. *Mol Biol Cell.* 2004;15(9):4043–4050. doi:10.1091/mbc.e04-05-0402

56. Tang W, Hemler ME. Caveolin-1 regulates matrix metalloproteinases-1 induction and CD147/EMMPRIN cell surface clustering. *J Biol Chem.* 2004;279(12):11112–11118. doi:10.1074/jbc.M312947200
57. Madaro L, Antonangeli F, Favia A, et al. Knock down of caveolin-1 affects morphological and functional hallmarks of human endothelial cells. *J Cell Biochem.* 2013;114(8):1843–1851. doi:10.1002/jcb.24526
58. Jin X, Sun Y, Xu J, Liu W. Caveolin-1 mediates tissue plasminogen activator-induced MMP-9 up-regulation in cultured brain microvascular endothelial cells. *J Neurochem.* 2015;132(6):724–730. doi:10.1111/jnc.13065
59. Théry C, Witwer KW, Aikawa E, et al. Minimal information for studies of extracellular vesicles 2018 (MISEV2018): a position statement of the International Society for Extracellular Vesicles and update of the MISEV2014 guidelines. *J Extracell Vesicles.* 2018;7(1):1535750. doi:10.1080/20013078.2018.1535750

International Journal of Nanomedicine

Dovepress

### Publish your work in this journal

The International Journal of Nanomedicine is an international, peer-reviewed journal focusing on the application of nanotechnology in diagnostics, therapeutics, and drug delivery systems throughout the biomedical field. This journal is indexed on PubMed Central, MedLine, CAS, SciSearch<sup>®</sup>, Current Contents<sup>®</sup>/Clinical Medicine, Journal Citation Reports/Science Edition, EMBase, Scopus and the Elsevier Bibliographic databases. The manuscript management system is completely online and includes a very quick and fair peer-review system, which is all easy to use. Visit <http://www.dovepress.com/testimonials.php> to read real quotes from published authors.

Submit your manuscript here: <https://www.dovepress.com/international-journal-of-nanomedicine-journal>